Selective miRNA disruption in T reg cells leads to uncontrolled autoimmunity

Xuyu Zhou,[1] Lukas T. Jeker,[1] Brian T. Fife,[1] Shirley Zhu,[1] Mark S. Anderson,[1,2] Michael T. McManus,[1,3] and Jeffrey A. Bluestone[1,2,3]

[1]Diabetes Center, [2]Department of Medicine, and [3]Department of Microbiology and Immunology, University of California, San Francisco (UCSF), San Francisco, CA 94143

A new regulatory T (T reg) cell–specific, FoxP3-GFP-hCre bacterial artificial chromosome transgenic mouse was crossed to a conditional Dicer knockout (KO) mouse strain to analyze the role of microRNAs (miRNAs) in the development and function of T reg cells. Although thymic T reg cells developed normally in this setting, the cells showed evidence of altered differentiation and dysfunction in the periphery. Dicer-deficient T reg lineage cells failed to remain stable, as a subset of cells down-regulated the T reg cell–specific transcription factor FoxP3, whereas the majority expressed altered levels of multiple genes and proteins (including Neuropilin 1, glucocorticoid-induced tumor necrosis factor receptor, and cytotoxic T lymphocyte antigen 4) associated with the T reg cell fingerprint. In fact, a significant percentage of the T reg lineage cells took on a T helper cell memory phenotype including increased levels of CD127, interleukin 4, and interferon γ. Importantly, Dicer-deficient T reg cells lost suppression activity in vivo; the mice rapidly developed fatal systemic autoimmune disease resembling the FoxP3 KO phenotype. These results support a central role for miRNAs in maintaining the stability of differentiated T reg cell function in vivo and homeostasis of the adaptive immune system.

CORRESPONDENCE
Jeffrey A. Bluestone:
jbluest@diabetes.ucsf.edu

Regulatory T (T reg) cells play an essential role in controlling autoimmunity (1). The absence of T reg cells in mice and humans because of a deficiency in the forkhead transcription factor FoxP3 leads to multiorgan autoimmune disease (2–5). The vital function of $FoxP3^+$ T cells in maintaining normal immune homeostasis is demonstrated by the fatal consequence of depletion of these cells in normal adult mice (6). Peripheral function, stability, and survival of T reg cells are essential to maintain immune homeostasis. Defects in IL-2 production or IL-2 receptor expression interfere with the peripheral survival of T reg cells and lead to the loss of self-tolerance (7). Similarly, blockade of the CD28–B7 pathway in autoimmune-prone, nonobese diabetic mice leads to exacerbated autoimmunity (8). This autoimmunity affects multiple organs, including pancreatic islets, exocrine pancreas, salivary glands, thyroid, and peripheral nervous tissues (1). Thus, T reg cells are essential to the maintenance of self-tolerance and the prevention of both organ-specific and systemic autoimmune diseases.

MicroRNAs (miRNAs) are small, single-stranded RNA molecules (21–22 nucleotides in length) with the potential to regulate endogenous gene expression in immune homeostasis (9, 10). miRNAs are transcribed as long transcripts (pri-miRNAs), cropped into hairpin-shaped pre-miRNAs, and processed by Dicer into the short RNAs that are responsible for the post-transcriptional regulation of expression of multiple mRNAs and, hence, protein. Thus, the elimination of Dicer abolishes miRNA production and subsequent function (11).

Previous studies (12) have demonstrated that miRNAs play an important role in the thymic development of T reg cells. However, the involvement of miRNAs after T reg lineage commitment was less clear because effector T (Teff) cells with dysregulated miRNAs are functionally impaired or even prone to autoimmunity through a mechanism involving miRNA-mediated mRNA decay (13).

The online version of this article contains supplemental material.

The Rockefeller University Press $30.00
J. Exp. Med. Vol. 205 No. 9 1983-1991
www.jem.org/cgi/doi/10.1084/jem.20080707

In this report, we test the role of miRNAs in mature T reg cell function by crossing a FoxP3-GFP-hCre transgenic (Tg) mouse to a conditional Dicer knockout mouse (*Dicer*$^{lox/lox}$) to inactivate miRNA generation selectively in T reg cells (14). Disruption of Dicer in T reg cells at the time of first FoxP3 expression did not affect thymic T reg cell development. However, the peripheral miRNA-deficient T reg cells rapidly adopt an effector-like phenotype with overlapping features of Th1, Th2, and T reg cells, and altered cytokine profiles and cell-surface expression of T reg cell markers, and they failed to stably express FoxP3. The T reg cell–specific FoxP3-GFP-hCre *Dicer*$^{lox/lox}$ KO mice rapidly develop spontaneous systemic autoimmune disease similar to the disease observed in T reg cell–deficient FoxP3 KO mice.

RESULTS AND DISCUSSION

Generation of bacterial artificial chromosome (BAC) Tg mice that enable GFP and Cre recombinase expression in FoxP3$^+$ cells

We developed a Foxp3 promoter–driven BAC Tg mouse strain that carries a fusion protein containing GFP fused to the N-terminus of a codon-optimized hCre (see Materials and methods; Fig. 1 A). Phenotypic analyses of the Tg mice showed that GFP$^+$ cells were uniformly CD4$^+$, with the majority CD25^{bright} and CD127^{low} (Fig. 1 B), as previously described for the T reg cell subset (15). The GFP$^+$ T cells were overwhelmingly FoxP3$^+$ based on intracellular staining of endogenous FoxP3 in the LN, spleen, and thymus (Fig. 1 C). Functional activity of Cre was tested by breeding the Cre Tg mouse line to a yellow fluorescent protein (YFP) reporter mouse, termed ROSA26R-YFP (16). The majority of GFP$^+$ cells from the LNs of FoxP3-GFP-hCre × ROSA26R-YFP mice were YFP$^+$ cells, as noted by the fact that the overall fluorescence intensity of YFP was a log greater than the GFP signal (Fig. S1 A, available at http://www.jem.org/cgi/content/full/jem.20080707/DC1). Two-color analyses of GFP and YFP further showed that >95% of the GFP$^+$ cells in the LN (Fig. 1 D) and spleen were YFP$^+$, demonstrating the high specificity and efficiency of the FoxP3-GFP-hCre mice. However, a subset of ~10% T reg cells spontaneously lost FoxP3 expression in vivo in healthy wild-type animals (Fig. 1 D). We were unable to distinguish whether the YFP$^+$ GFP$^-$ cells have transiently expressed FoxP3 (as has been found in human T cells) or were a consequence of unstable T reg cells (bona fide T reg cells that have lost Foxp3). However, similar observations have been made by using a FoxP3-cre knock-in system; thus, we are confident that this is not an artifact of our BAC Tg system (17, 18).

Selective Dicer disruption in T reg cells

To address the role of miRNAs directly in T reg cells, the FoxP3-GFP-hCre mice were bred to a conditional *Dicer*^{loxlox} mouse (14), in some cases together with an ROSA26R-YFP allele, as indicated in the figures. Genomic PCR analysis was used to assess Dicer deletion in T reg cells (Fig. S1, A and B). CD4$^+$ YFP$^+$ cells from *Dicer*$^{wt/lox}$ mice (Dicer Het) displayed only a wild-type band, suggesting that the *Dicer* locus was sensitive to Cre recombination and was efficiently deleted in T reg cells. Further evidence for efficient Dicer deletion in T reg cells was based on real-time PCR analyses to quantify floxed *Dicer* alleles. The level of the floxed *Dicer* allele in YFP$^+$ T reg cells from homozygous *Dicer*$^{lox/lox}$ KO mice was <10% of the control levels found in the mouse tails and sorted CD4$^+$GFP/YFP$^-$ non–T reg cells from the same animal. Finally, we observed

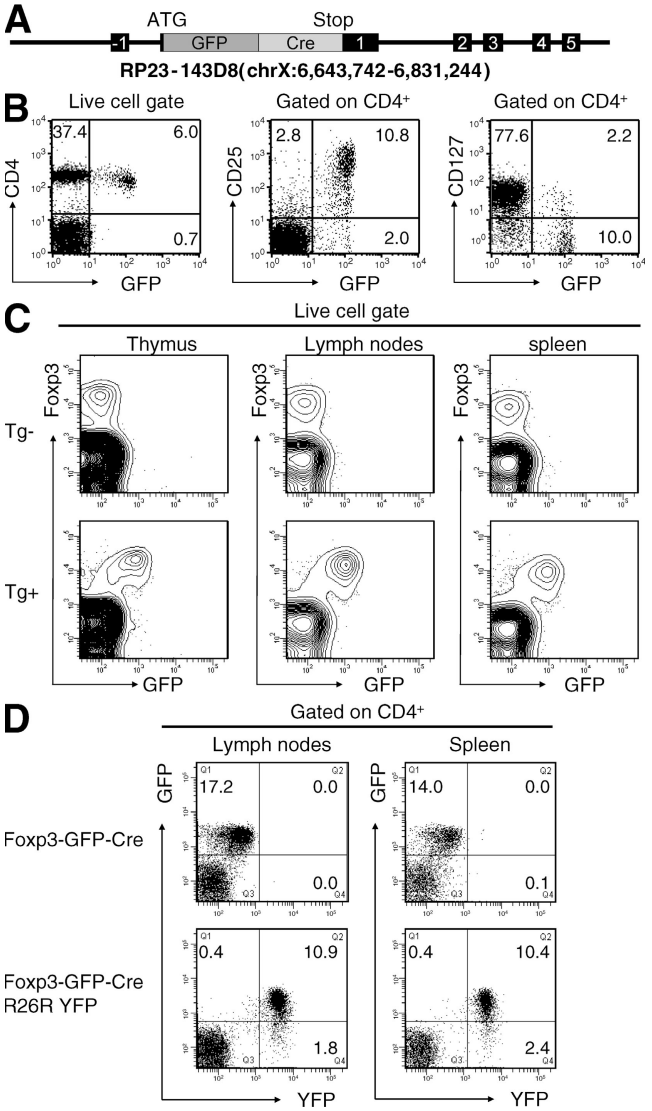

Figure 1. Generation of FoxP3-GFP-hCre BAC Tg mice. (A) The final BAC Tg construct used for generating mice. (B) Flow cytometric analysis of LN cells from 8-wk-old Tg mice indicated specific transgene expression in CD4$^+$CD25^{high}CD127^{low} T cells. The percentage of cells in each quadrant is indicated. (C) Intracellular FoxP3 staining revealed that GFP expression in the thymus, LN, and spleen was restricted to FoxP3$^+$ cells. (D) To monitor hCre activity in vivo, FoxP3-GFP-hCre Tg mice were crossed to YFP reporter mice. Flow cytometric analysis of GFP or YFP expression in CD4 T cells from LN or spleen shows specific and efficient reporter activation. The percentage of cells in each gated population is indicated.

a substantial decrease in the levels of two representative mature miRNAs, miR15b and miR142-5b, in the homozygous mice in the LN $CD4^+YFP^+$ cells, consistent with efficient miRNA elimination in Dicer-deficient T reg cells (Fig. S1 C). Collectively, these results suggested that the Cre recombinase was active and selectively deleted the critical Dicer RNaseIII2 domain, leading to a subsequent loss of miRNAs in $FoxP3^+$ and their progeny cells.

Phenotypic analysis of conditional Dicer-deficient T reg cells

2-wk-old mice were examined for changes in T reg cell development in the thymus, a phenotype previously observed in conditional Dicer KO mice bred to Lck-Cre or CD4-Cre strains (12). There was no difference in the percentages of the individual $CD4^+CD8^+$ double-positive thymocytes, as well as $CD4^+$ and $CD8^+$ single-positive (SP) T cells, consistent with the highly specific expression and function of FoxP3-driven Cre (Fig. 2 A). There was an equal percentage and absolute number of T reg cells in the thymus when the control *Dicer*$^{wt/lox}$ mice (Dicer Het) were compared with *Dicer*$^{lox/lox}$ (Dicer KO) FoxP3-GFP-hCre mice, based on both expression of GFP and FoxP3 protein analyses (Fig. 2 A, bottom; and not depicted). Similar results were observed in the LN and spleen of mice <2 wk of age (Fig. 2 B). The percentages of $FoxP3^+$ T reg cells were equivalent in *Dicer*$^{wt/lox}$ versus *Dicer*$^{lox/lox}$ KO animals. There was no evidence of increased apoptosis and only minimal changes in the proliferation of the T reg cell subset based on flow cytometric DNA analyses (unpublished data). These data suggest that deletion of Dicer at the time of FoxP3 expression had minimal effects on T reg cell development, seeding, proliferation, and survival in the peripheral compartments.

Splenomegaly and lymphadenopathy were noted in all aging FoxP3-GFP-hCre *Dicer*$^{lox/lox}$ mice (Fig. 3 A). Although there was a dramatic increase in the total number of LN and splenic T cells in 4–6-wk-old Dicer KO versus Dicer Het animals, the percentages of T reg cells ($FoxP3^+$) were largely maintained in LN and were reduced to 33% in the spleen and peripheral blood (Fig. 3 B, right; and not depicted). A much more dramatic reduction of the percentage of T reg cells was found in the mixed BM chimeras, in which conditional KO BM cells are transferred together with WT BM cells isolated from congenic Thy1.1 mice into sublethally irradiated Rag KO hosts (not depicted). These results suggest that Dicer KO cells compete poorly with the WT T reg cells, consistent with an earlier observation demonstrating similar T reg cell instability in a FoxP3-attenuated mouse model (19).

$CD4^+FoxP3^+$ T reg cells from Dicer KO mice appeared more "activated," as there was an overall increase in the mean fluorescence of CD25, cytotoxic T lymphocyte antigen 4 (CTLA4), CD69, and glucocorticoid-induced TNFR. In addition, the Dicer KO T reg cells contained a higher percentage of $CD103^+$ T cells and significantly more $CD62L^{lo}$ cells (Fig. 3 C).

Dicer-deficient T reg cells are not a stable lineage

Transcript microarray analyses were performed on RNA extracted from sorted $CD4^+YFP^+$ T cells (>95% pure) isolated from LNs of 1-mo-old Dicer Het versus Dicer KO mice (Fig. S1 A). Based on a *t* test with cutoff p-values of <0.05, and a fold change of >2, 686 probe sets were found to be differentially regulated in these two populations (Fig. 4 A; and Table S1, available at http://www.jem.org/cgi/content/full/jem.20080707/DC1). 481 probe sets (393 genes) were observed to be up-regulated in Dicer KO T reg cells.

Several well-documented genes involved in IFN-γ production increased in Dicer KO YFP^+ cells, including T-bet, the master regulator of Th1 cells, and Eomes, a paralogue of T-bet. Previous studies (20) have shown that ectopic expression

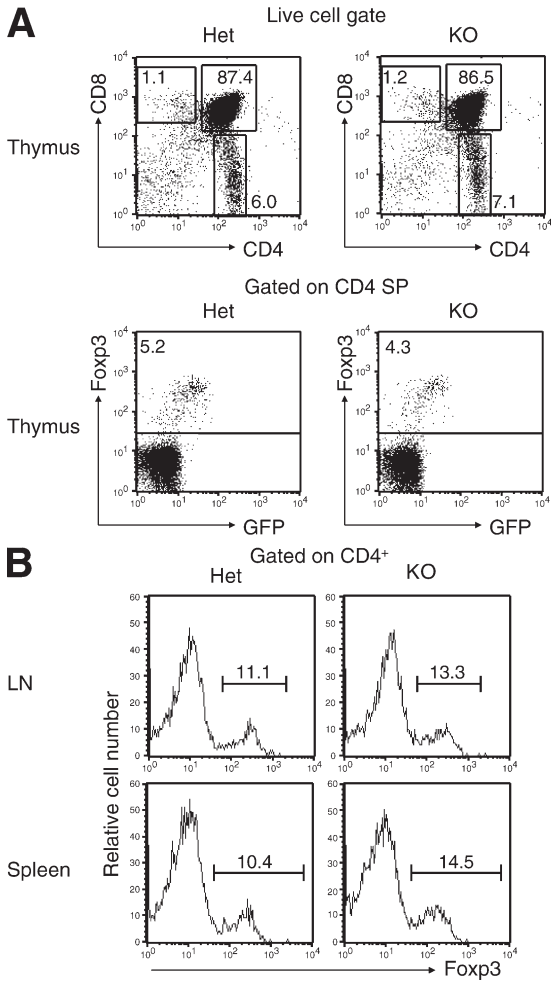

Figure 2. Normal thymic T reg cell development and seeding of the peripheral compartments in the FoxP3-hCre *Dicer*$^{lox/lox}$ model. (A) Flow cytometric analysis was performed on 2-wk-old FoxP3-GFP-hCre *Dicer*$^{wt/lox}$ (Het) and FoxP3-GFP-hCre *Dicer*$^{lox/lox}$ (KO) mice for CD4, CD8, and FoxP3 expression. $CD4^+$ SP thymocytes were analyzed for concomitant GFP and FoxP3 expression, illustrating equal relative expression of $FoxP3^+$ cells in the thymus in Dicer wild-type and Dicer-deficient T reg cells. The percentage of cells in each gate is indicated. (B) Similar results to A were obtained in the LN and spleen.

of Eomes was sufficient to induce IFN-γ. Interestingly, Eomes also regulates granzyme B (20), another gene found to be highly dysregulated in the Dicer KO YFP$^+$ but also KO GFP$^+$ cells (Fig. 4 C). Finally, other related genes including, Runx3, another Th1-specific transcription factor that cooperates with T-bet to enforce specification of the Th1 lineage (21), and GADD45 (22), which mediates the activation of the p38 and c-Jun N-terminal kinase mitogen-activated protein kinase pathways and IFN-γ, were also elevated. Development of the Teff cell phenotype and dysregulation of the IFN-γ pathway has been shown in the FoxP3 KO cells marked by a FoxP3 promoter–driven GFP transgene (23). In fact, a comparison of the genes expressed differentially in Dicer Het versus Dicer KO T reg cells and FoxP3$^+$ WT versus FoxP3$^+$ KO T reg cells showed a significant overlap. Among the ∼650 differentially regulated genes, ∼100 genes (112 probe sets) were dysregulated in FoxP3-deficient T reg cells (Fig. 4 A; and Table S2, available at http://www.jem.org/cgi/content/full/jem.20080707/DC1). Most notably, the expression of the T reg cell transcriptional program often linked to Teff cells (including Gzma, Gzmk, Gzmb, Il4, Ccl1, Runx2, Ccr5, Cxcl10, Tbx21, and IFN-γ) was up-regulated in both KO cell types (Fig. 4 A).

One important function of FoxP3 is stabilization of the T reg lineage through a positive feedback loop that enhances FoxP3 expression (24). Therefore, we tested T reg lineage stability in Dicer KO mice by examining the expression of FoxP3 in conditional Dicer KO versus Dicer Het T reg cells marked by expression of YFP. Approximately 89% (ranging from 86–94%) of the CD4$^+$YFP$^+$ cells isolated from Dicer Het mice express FoxP3 at 4–7 wk of age, based on both GFP and FoxP3$^+$ protein (Fig. 1 D and Fig. 4 B; and Fig. S2, available at http://www.jem.org/cgi/content/full/jem.20080707/DC1). In contrast, a mean of 38% (ranging from 17–52%) of CD4$^+$YFP$^+$ cells from the Dicer KO mice were FoxP3$^-$ (Fig. 4 B), a phenotype resembling the FoxP3-deficient T reg cells. There was a clear correlation between age and the increase in the number of CD4$^+$YFP$^+$Foxp3$^-$ cells (Fig. S2).

The gene expression profile of the Dicer KO YFP$^+$ T cells might reflect either the dysregulation of FoxP3 function and/or the loss of FoxP3 expression by a significant subset of the FoxP3 lineage cells. It was unlikely that the differential gene expression was coming from the FoxP3 protein–negative population, because the microarray experiment was done using Dicer KO mice in which ∼80% YFP$^+$ cells were Foxp3$^+$. Indeed, the expression of multiple genes (including Neuropilin-1, IFN-γ, IL-10, GADD45, CCR5, Satb1, and Gzmb) was altered in the miRNA-deficient GFP$^+$ T reg cells isolated from either Dicer Het or Dicer KO mice (Fig. 4 C). Expression of Neuropilin-1 and GPR83 (unpublished data), both quintessential FoxP3-dependent T reg cell markers, were down-regulated in conditional Dicer KO T reg cells. In contrast, IFN-γ, IL-10, and granzyme B (Fig. 4 C), as well as IL-4, GADD45, CCR5, and Satb1 (not depicted), were highly expressed in the Dicer KO FoxP3$^+$ T reg cells. IFN-γ expression was further confirmed by intracellular staining. Almost 5% of Dicer KO CD4$^+$GFP$^+$ cells, treated with PMA and ionomycin in the presence of monensin, expressed IFN-γ as

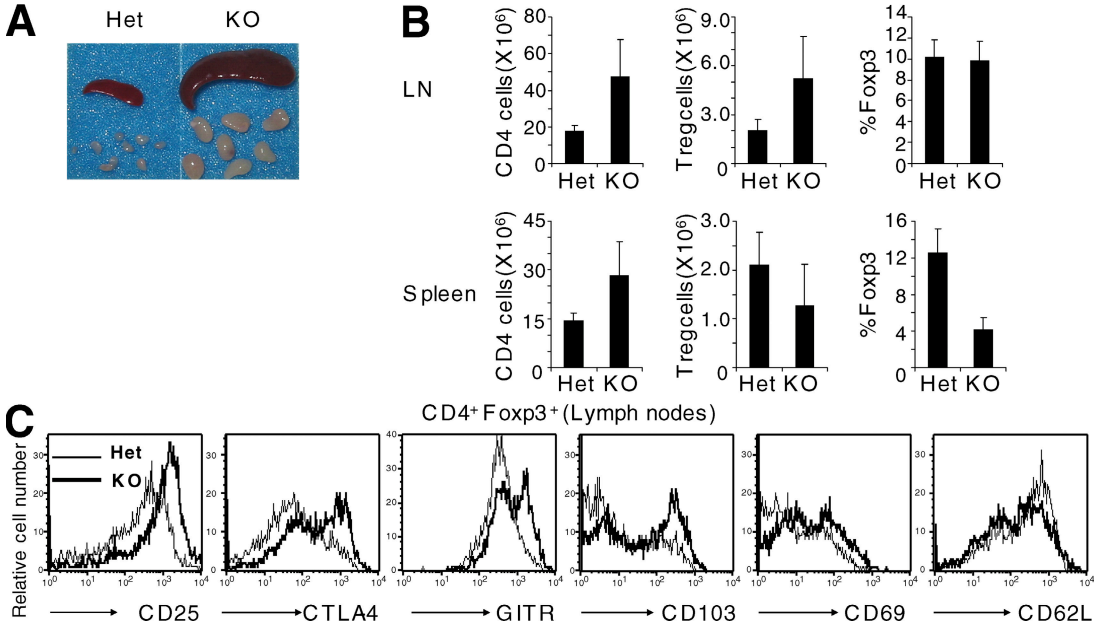

Figure 3. Phenotype of miRNA-deficient T reg cells. (A) Splenomegaly and lymphadenopathy in >5-wk-old FoxP3-GFP-hCre *Dicer*$^{lox/lox}$ (KO) mice. Data are representative of >10 mice. (B) LN and spleen T cell subsets in 4–6-wk-old mice. Absolute numbers of CD4$^+$FoxP3$^-$ and CD4$^+$FoxP3$^+$ cells were calculated by multiplying the percentage of cells determined by FACS by the absolute cell number per tissue. Data represent means ± SD (n = 5). (C) LNs were harvested at 5 wk from FoxP3-GFP-hCre *Dicer*$^{wt/lox}$ (Het) and FoxP3-GFP-hCre *Dicer*$^{lox/lox}$ (KO) mice and analyzed for the indicated cell-surface markers gated on CD4$^+$FoxP3$^+$ lymphocytes.

compared with <0.6% in Dicer Het T reg cells (Fig. 4 D). Interestingly, we observed dysregulation of another FoxP3-regulated protein, CD127, on the FoxP3$^+$ Dicer KO T reg cell population (Fig. 4 E). The dysregulation of IFN-γ, Neuropilin-1, and CD127 in cells expressing FoxP3 indicated that independent or downstream targets of Foxp3 are functionally defective in the absence of miRNAs.

Up-regulation of genes in the Dicer KO cells could be a direct result of the loss of relevant mature miRNAs, which control gene expression through binding to the 3′ untranslated

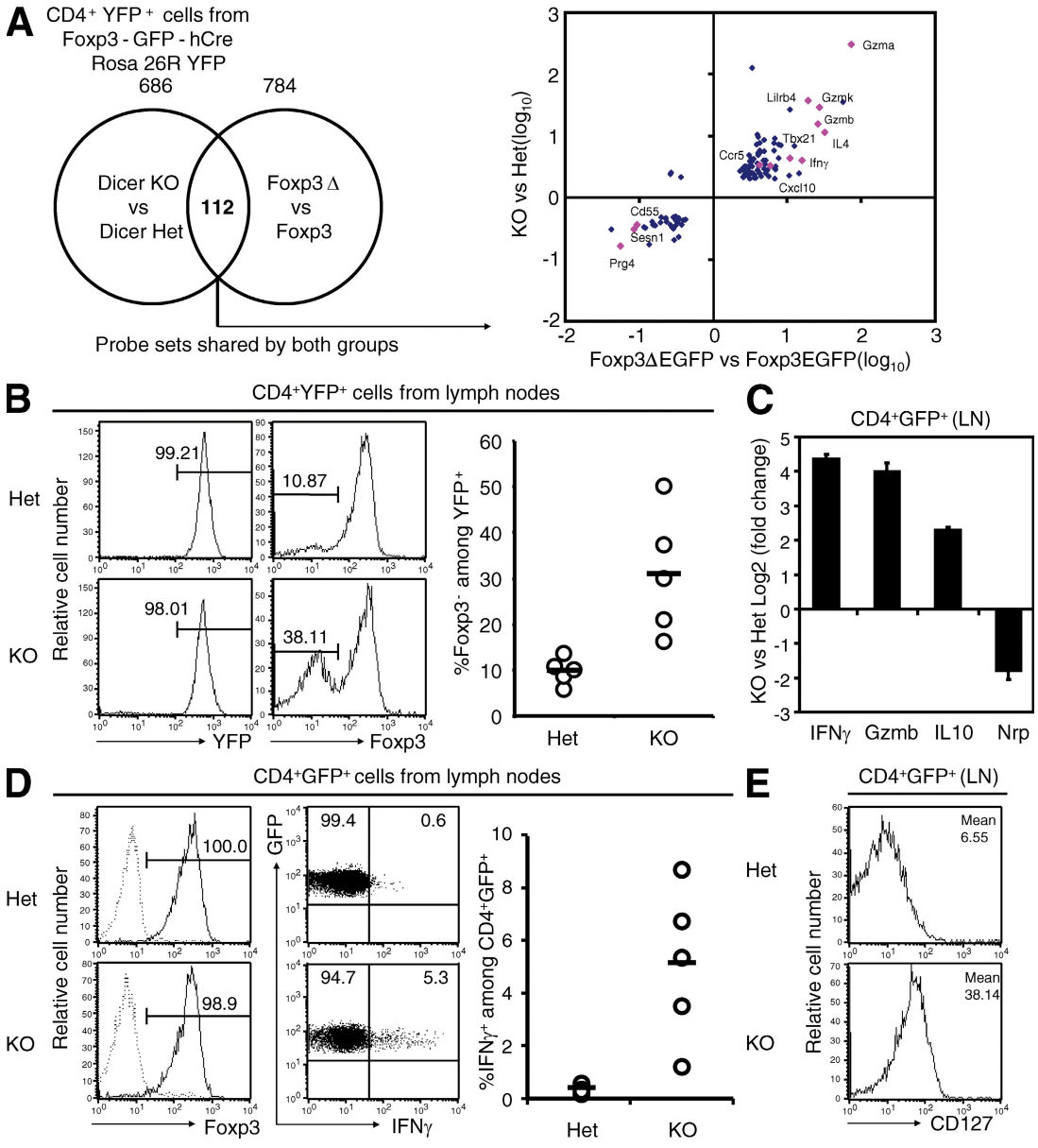

Figure 4. miRNA-dependent T reg lineage stability. (A) Overlap of the gene expression profile of Dicer KO T reg cells and FoxP3-deficient T reg cells. LN CD4$^+$YFP$^+$ T cells (>95% pure) from FoxP3-GFP-hCre × ROSA26R-YFP *Dicer*$^{wt/lox}$ (Het) and FoxP3-GFP-hCre × ROSA26R-YFP *Dicer*$^{lox/lox}$ (KO) mice (~30 d old) were isolated by flow cytometry. The genes expressed differentially in Dicer KO versus Het T reg cells were compared with the published data of FoxP3 KO versus FoxP3$^+$ T reg cells (reference 23). Two-dimensional scatter plot of those common gene expression values is shown. Gzma, Lilrb4, Gzmk, Gzmb, Tbx21, INF-γ, Cxcl10, Ccr5, Cd55, IL4, Sesn1, and Prg4 are highlighted. (B) FoxP3 expression in sorted CD4$^+$YFP$^+$ cells was examined by flow cytometry analysis. Numbers on bracketed lines indicate the percentage of cells in each gated population. Each symbol represents one mouse (from 4 to 7 wk). Small horizontal lines indicate the mean. (C) Levels of mRNA for the indicated genes in CD4$^+$GFP$^+$ (FoxP3-expressing cells) from 5-wk-old FoxP3-GFP-hCre *Dicer*$^{lox/lox}$ (KO) mice were determined by real-time PCR analysis. Data represent the mean ± SD. (D) IFN-γ production was examined by intracellular cytokine staining. FoxP3 expression in CD4$^+$GFP$^+$ was confirmed by intracellular FoxP3 staining (left, continuous lines); dotted lines indicate CD4$^+$GFP$^-$ cells. (right) The percentage of IFN-γ cells from several Het and KO mice. Each symbol represents one 4–6-wk-old mouse. Small horizontal lines indicate the mean. (E) CD127 expression of the same cell subset is shown. Mean, mean fluorescence intensity.

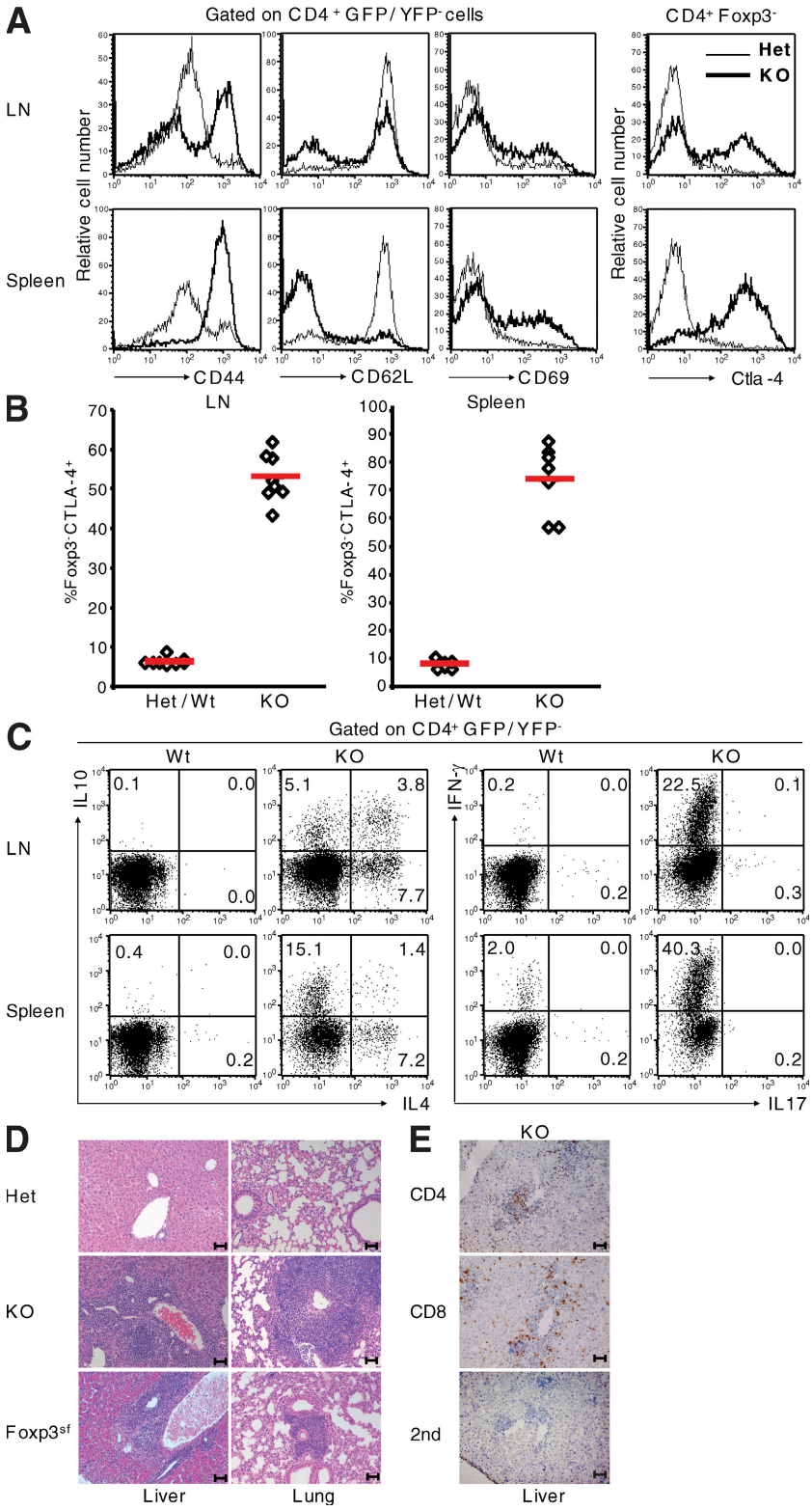

Figure 5. T reg cell–specific Dicer ablation results in the loss of suppressor function in vivo. (A) Flow cytometric analysis of activation markers on Teff cells reveals strong activation of nonregulatory (GFP^-YFP^-) cells. LN and spleen cells from 5-wk-old FoxP3-GFP-hCre × ROSA26R-YFP *Dicer*$^{wt/lox}$ (Het) and FoxP3-GFP-hCre × ROSA26R-YFP *Dicer*$^{lox/lox}$ (KO) mice were stained for CD4 and the indicated proteins. Teff cells were gated on $CD4^+GFP^-/YFP^-$ lymphocytes and analyzed for CD44, CD62L, and CD69 expression. For analysis of intracellular CTLA4, cells were stained with FoxP3 antibody and gated on $FoxP3^-$ cells to distinguish T reg cells from Teff cells. (B) Percentage of $CD4^+CTLA4^+FoxP3^-$ Teff cells from wild-type and KO mice (4–6 wk old) from LNs and spleen. Each symbol represents one mouse. Small horizontal lines indicate the mean. (C) Flow cytometric analysis illustrates massive cytokine production

region sequence. T reg cells and conventional CD4+ T cells have different miRNA profiles (12). Therefore, we mined relevant T reg cell–specific mRNA expression data to determine if their up-regulation correlated with the presence of predicted miRNA binding sites to a selected set of miRNAs preferentially expressed in T reg cells (miR-15b, miR-16, miR-21, miR-22, miR-23a, miR-23b, miR-24, miR-27b, miR-29c, miR-30a, miR-103, miR-125a-3p, miR-146a, miR-149, miR-155, miR-191, miR-207, miR-214, miR-223, and miR-297a). We used miRDB, an miRNA target prediction and functional annotation database (25). Of 393 genes that were observed to be up-regulated in Dicer KO T reg cells, 114 genes (29%) have potential target sites for the regulated miRNAs. These include several key genes such as CD127, IFN-γ, Eomes, Socs3, Runx2, FasL, and Smurf2 (Table S3, available at http://www.jcb.org/cgi/content/full/jcb.20080707/DC1). Down-regulation of CD127 and IFN-γ in T reg cells is Foxp3 dependent (26), yet Dicer KO T reg cells express high levels of IFN-γ and CD127 even in cells expressing FoxP3. It is interesting to note that these genes have binding sites for the miRNAs found by Cobb et al. (12) to be overexpressed in T reg cells (miR-214 and miR-27b for CD127, and miR-27b for IFN-γ). These results strongly suggest that additional regulation might occur through miRNAs that act downstream of Foxp3 in the regulation of this gene product.

T reg cell–specific Dicer ablation results in the loss of suppressor function in vivo

Aging FoxP3-GFP-hCre Dicer KO mice began to resemble FoxP3 KO mice. The majority of LN and splenic CD4+YFP− or FoxP3− T cells from Dicer KO mice down-regulated CD62L expression and increased expression of CD44, CD69, and CTLA4, consistent with an activated phenotype (Fig. 5 A). The number of CTLA4-expressing CD4+FoxP3− effectors increased from <10% of splenic and LN CD4+ T cells in Dicer Het and *Dicer*$^{wt/wt}$ (Wt) littermates to >50 and >70% in Dicer KO LNs and spleens, respectively (Fig. 5 B). Intracellular cytokine production was assessed in the PMA plus ionomycin–activated CD4+YFP− T cells from FoxP3-GFP-hCre × ROSA26R-YFP Dicer wild-type or Dicer KO mice. Less than 1% of the LN or splenic T cells from control mice expressed IL-10, IL-4, IFN-γ, or IL-17. In sharp contrast, a significant percentage of Teff cells (YFP−) from T reg cell–specific Dicer KO mice expressed high levels of IL-4, IL-10, and, especially, IFN-γ (Fig. 5 C). Thus, the increased effector function was secondary to the miRNA defect, which was limited to only the T cells that expressed or had once expressed FoxP3.

All of the conditional Dicer KO mice were dead by 6–8 wk of age. Clinical signs of disease included weight loss, reduced mobility, and a hunched back. Both lung and liver tissues were extensively infiltrated with mononuclear cells similar to the infiltrates observed in the FoxP3 KO mouse (Fig. 5 D). Lungs of both Scurfy and Dicer KO tissue exhibited dense, predominantly peribronchovascular mononuclear infiltrates (Fig. 5 D), consistent with an autoimmune disease. The infiltrate was composed of both CD4+ and CD8+ T cells, not unlike what has been observed in other T reg cell–dependent lymphoproliferative diseases and FoxP3-deficient mice (Fig. 5 E).

In summary, these results demonstrate that miRNAs are essential in maintaining FoxP3 expression and controlling lineage specificity within the T reg cell subset. The newly generated FoxP3-GFP-hCre mouse strain allowed us to focus on the peripheral effects of miRNA disruption, because Dicer deletion occurred only after the T cells had fully committed to the T reg lineage. The specific loss of miRNA processing led to a severe T reg cell dysfunction in the periphery, leading to a high morbidity and mortality at 4–8 wk of age, which reveals the central role of miRNAs in controlling T reg cell function in vivo. T reg cell–specific miRNA ablation resulted in a much more aggressive lymphoproliferative disease than miRNA ablation in all CD4+ T cells and closely resembled the Scurfy phenotype (12). The relatively mild disease found in the CD4-Cre × *Dicer*$^{lox/lox}$ mouse strain suggests a role of miRNAs in regulating the activation, migration, and/or function of conventional T cells, thus masking the severity of the T reg cell defect caused by impaired conventional T cell function. Dicer-deficient T reg cells failed to keep the T reg lineage stable and also developed a Teff cell–like phenotype. Strikingly, the YFP+ or GFP+ cells isolated from T reg cell–specific FoxP3-GFP-hCre *Dicer*$^{lox/lox}$ KO mice produced IFN-γ and expressed a memory cell marker, which indicated that some of the FoxP3 functions might be defective in the absence of miRNAs. The detailed study of which miRNAs are directly involved in T reg cell stability remains to be defined. However, there have been a large number of miRNAs that have been identified in T reg cells, including some that are differentially expressed in this subset and regulated by Foxp3 (12, 27). Many potential gene targets of the T reg cell–enriched miRNAs increased after Dicer ablation, including CD127 (a predicted target of miR-214 and miR-27b) and IFN-γ (miR-27b), even in Foxp3+ cells. These results support the notion that at least some miRNAs act downstream of Foxp3 in T reg cells to control autoimmunity.

The detailed mechanism of how miRNAs regulate T reg cell function remains a key question for future studies. We have performed multiple in vitro suppression assays with the isolated T reg cells from Dicer KO mice and have observed variable results. The function appeared defective in only 50% of the assays performed. It is possible that the overexpression

by CD4+GFP−/YFP− effector cells from 5-wk-old FoxP3-GFP-hCre × ROSA26R-YFP Dicer KO but not FoxP3-GFP-hCre × ROSA26R-YFP Dicer wild-type mice. The percentage of cells in each quadrant is indicated. (D) Paraffin-embedded histological sections of lung and liver from 5-wk-old mice were fixed and stained with hematoxylin and eosin ($n > 5$). (E) Frozen sections of the FoxP3-GFP-hCre *Dicer*$^{lox/lox}$ (KO) mice in D were stained for the presence of CD4+ and CD8+ T cells. Visualization was done with DAB substrate (Vector Laboratories) and was followed by hematoxylin counterstain. Bar, 50 µm.

of IL-10 and Gzms in the Dicer KO T reg cells might mask the functional defect in this in vitro assay (Fig. 4 C). The decreased Neuropilin-1 expression in the Dicer KO Foxp3$^+$ T reg cells (Fig. 4 C) might provide an alternative explanation, because Neuropilin-1 contributes to the prolonged interaction of T reg cells with dendritic cells in vivo (28). Indeed we found much higher CD40 expression on the dendritic cells from Dicer KO mouse (unpublished data), similar to the DC activation observed after T reg cell ablation (6). It is unlikely that the lymphoproliferative disease is the result of generated YFP$^+$Foxp3$^-$ cells in the Foxp3-Cre Dicer KO mouse. First, the majority of the T cells expressing the activated phenotype were both YFP$^-$ and Foxp3$^-$ (Fig. 5 A). Second, it seems unlikely that the limited decrease in the percentage of Foxp3 cells in Dicer KO mice is sufficient to lead to pathology. Third, the much milder disease found in the CD4-Cre × *Dicer*$^{lox/lox}$ mouse strain suggests that Teff cells are functionally impaired in absence of miRNAs (12).

MATERIALS AND METHODS

Generation of T reg cell–specific Dicer conditional KO mice. The GFP-hCre cDNA fragment was inserted immediately downstream of the FoxP3 ATG translational start site by homologous recombination into a 188-kb mouse BAC (from the C57BL/6 genome; clone RP23-143D8) carrying the intact FoxP3 gene, as previously described (29). We used a codon-optimized "humanized" Cre (hCre) to improve translational efficiency in eukaryotic cells. An *EGFP-hcre-Frt-Neo-Frt* cassette was provided by N. Killeen (UCSF, San Francisco, CA). The modified BAC was purified using cesium chloride gradient ultracentrifugation and microinjected by the UCSF Transgenic/Targeted Mutagenesis Core Facility into the pronuclei of nonobese diabetic mouse embryos to generate FoxP3-GFP-hCre BAC Tg mice. Mice carrying the GFP-hCre transgene were screened by FACS analysis using peripheral blood cells. Several founder mice were generated and screened for GFP expression and lack of functional FoxP3 protein, as indicated by an inability of the transgene to rescue the FoxP3 KO mice. *Dicer*$^{lox/lox}$ (14) mice and ROSA26R-YFP reporter mice (16) have been previously described. All mice were housed and bred under specific pathogen-free conditions at the UCSF Animal Barrier Facility. All animal experiments were approved by the Institutional Animal Care and Use Committee of UCSF.

Antibodies. Labeled antibodies specific for CD4 (RM4-5), CD8 (Ly-2), CD25 (PC61), glucocorticoid-induced TNFR (DTA-1), CD62L (MEL14), CD69 (H1.2F3), CD103 (M290), CD127 (A7R34), CD152 (UC10-4F10), FoxP3 (FJK-16s), and IFN-γ (XMG1.2) were purchased from BD Biosciences or eBioscience.

Flow cytometry. Stained single-cell suspensions were analyzed with a FACSCalibur analyzer running CellQuest software, or an LSRII flow cytometer and FACSDiva (BD Biosciences). T reg cells were sorted using a MoFlo cytometer high speed cell sorter (Dako) or FACSAria (BD Biosciences). A 510/20-nm filter (495LP dichroic mirror) and a 560/40-nm filter (535LP dichroic mirror) were used to discriminate the GFP from the YFP signal, respectively.

Gene expression profiling and analysis. CD4$^+$YFP$^+$ (>95% pure) cells from ∼30-d-old mice were purified by flow cytometry, and total RNA was isolated using TRIzol (Invitrogen). The biotinylated anti-sense RNA (aRNA) was generated using an aRNA amplification kit (MessageAmp II; Ambion). 15 μg of fragmented aRNA of each sample was applied onto the mouse 430 2.0 GeneChip (Affymetrix) for hybridization. Triplicate GeneChips were used for each T cell population. Analysis was conducted by GeneSpring GS.7.3.1 Gene Expression Analysis Software (Agilent Technologies). Statistically significant differences were analyzed using one-way analysis of variance when grouped by Dicer KO versus Dicer heterozygotes combined with the parametric test at variances not assumed equal (Welch *t* test), with a p-value cutoff of <0.05 followed by mean fold change cutoff of >2. Microarray data have been deposited in the Gene Expression Omnibus under accession no. GSE11818.

Real-time PCR analysis. Gene expression was measured in real time with a sequence detection system (GeneAmp 7900; Applied Biosystems). The TaqMan universal PCR Master Mix, and primers and probes for IL-10, Gzmb, Neuropilin-1, and GAPDH were purchased from Applied Biosystems. Primer sequences for IFN-γ were 5′-CATTGAAAGCCTAGAAAGTCTGAATAAC-3′ (forward) and 5′-TGGCTCTGCAGGATTTTCATG-3′ (reverse). The probe sequence for IFN-γ was 5′-FAMTCACCATCCTTTTGCCAGTTCCTCCAGTAMRA-3′ (Invitrogen). Data are presented and normalized to GAPDH using the comparative Ct method (ΔΔCt).

PCR analysis of Dicer KO mice. The conditional floxed allele was genotyped using primers DicerF1 (5′-CCTGACAGTGACGGTCCAAAG-3′) and DicerR1 (5′-CATGACTCTTCAACTCAAACT-3′), as previously described (15). The floxed allele produced a 420-bp PCR product, whereas a wild-type allele resulted in a 351-bp product and the deletion allele resulted in no PCR product. The same primers were used to quantitate the floxed *Dicer* alleles by real-time PCR with the SYBR green PCR Master Mix (Applied Biosystems). The FoxP3 promoter sequences 5′-CTGCTGCGAGTCTCTGAGTG-3′ (forward) and 5′-GGCCGCTATGTGTATGGTTT-3′ (reverse) were used for normalization.

Online supplemental material. Table S1 shows gene profiling of Dicer KO versus Dicer Het T reg cells. Table S2 shows overlap of the gene expression profile of Dicer KO T reg cells and FoxP3-deficient T reg cells. Table S3 provides miRNA target prediction in T reg cells. Fig. S1 shows the activity of hCre recombinase, and T reg cell–specific Dicer and miRNA ablation. Fig. S2 provides a kinetic analysis of Foxp3 stability in Dicer-deficient T reg cells. Online supplemental material is available at http://www.jem.org/cgi/content/full/jem.20080707/DC1.

The authors thank Dr. Nigel Killeen for microinjections, Shuwei Jiang for cell sorting, and Drs. Qizhi Tang and Abul Abbas for critical review of the manuscript.

L.T. Jeker was supported by the Swiss National Science Foundation (grant PBBSB-118644), the Roche Research Foundation, and the Freiwillige Akademische Gesellschaft Basel. X. Zhou was supported by an American Diabetes Association Mentor-Based Award. This work was supported by the National Institutes of Health (grants P01 AI35297-15, P30 DK63720, and U19 AI056388).

The authors have no conflicting financial interests.

Submitted: 3 April 2008
Accepted: 16 July 2008

REFERENCES

1. Tang, Q., and J.A. Bluestone. 2006. Regulatory T-cell physiology and application to treat autoimmunity. *Immunol. Rev.* 212:217–237.
2. Khattri, R., T. Cox, S.A. Yasayko, and F. Ramsdell. 2003. An essential role for Scurfin in CD4+CD25+ T regulatory cells. *Nat. Immunol.* 4:337–342.
3. Fontenot, J.D., M.A. Gavin, and A.Y. Rudensky. 2003. Foxp3 programs the development and function of CD4+CD25+ regulatory T cells. *Nat. Immunol.* 4:330–336.
4. Hori, S., T. Nomura, and S. Sakaguchi. 2003. Control of regulatory T cell development by the transcription factor Foxp3. *Science.* 299:1057–1061.
5. Brunkow, M.E., E.W. Jeffery, K.A. Hjerrild, B. Paeper, L.B. Clark, S.A. Yasayko, J.E. Wilkinson, D. Galas, S.F. Ziegler, and F. Ramsdell. 2001. Disruption of a new forkhead/winged-helix protein, scurfin, results in the fatal lymphoproliferative disorder of the scurfy mouse. *Nat. Genet.* 27:68–73.

6. Kim, J.M., J.P. Rasmussen, and A.Y. Rudensky. 2007. Regulatory T cells prevent catastrophic autoimmunity throughout the lifespan of mice. *Nat. Immunol.* 8:191–197.
7. Fontenot, J.D., J.P. Rasmussen, M.A. Gavin, and A.Y. Rudensky. 2005. A function for interleukin 2 in Foxp3-expressing regulatory T cells. *Nat. Immunol.* 6:1142–1151.
8. Salomon, B., D.J. Lenschow, L. Rhee, N. Ashourian, B. Singh, A. Sharpe, and J.A. Bluestone. 2000. B7/CD28 costimulation is essential for the homeostasis of the CD4+CD25+ immunoregulatory T cells that control autoimmune diabetes. *Immunity.* 12:431–440.
9. Thai, T.H., D.P. Calado, S. Casola, K.M. Ansel, C. Xiao, Y. Xue, A. Murphy, D. Frendewey, D. Valenzuela, J.L. Kutok, et al. 2007. Regulation of the germinal center response by microRNA-155. *Science.* 316:604–608.
10. Rodriguez, A., E. Vigorito, S. Clare, M.V. Warren, P. Couttet, D.R. Soond, S. van Dongen, R.J. Grocock, P.P. Das, E.A. Miska, et al. 2007. Requirement of bic/microRNA-155 for normal immune function. *Science.* 316:608–611.
11. Gregory, R.I., T.P. Chendrimada, N. Cooch, and R. Shiekhattar. 2005. Human RISC couples microRNA biogenesis and posttranscriptional gene silencing. *Cell.* 123:631–640.
12. Cobb, B.S., A. Hertweck, J. Smith, E. O'Connor, D. Graf, T. Cook, S.T. Smale, S. Sakaguchi, F.J. Livesey, A.G. Fisher, and M. Merkenschlager. 2006. A role for Dicer in immune regulation. *J. Exp. Med.* 203:2519–2527.
13. Yu, D., A.H. Tan, X. Hu, V. Athanasopoulos, N. Simpson, D.G. Silva, A. Hutloff, K.M. Giles, P.J. Leedman, K.P. Lam, et al. 2007. Roquin represses autoimmunity by limiting inducible T-cell co-stimulator messenger RNA. *Nature.* 450:299–303.
14. Harfe, B.D., M.T. McManus, J.H. Mansfield, E. Hornstein, and C.J. Tabin. 2005. The RNaseIII enzyme Dicer is required for morphogenesis but not patterning of the vertebrate limb. *Proc. Natl. Acad. Sci. USA.* 102:10898–10903.
15. Liu, W., A.L. Putnam, Z. Xu-Yu, G.L. Szot, M.R. Lee, S. Zhu, P.A. Gottlieb, P. Kapranov, T.R. Gingeras, B. Fazekas de St. Groth, et al. 2006. CD127 expression inversely correlates with FoxP3 and suppressive function of human $CD4^+$ T reg cells. *J. Exp. Med.* 203:1701–1711.
16. Srinivas, S., T. Watanabe, C.S. Lin, C.M. William, Y. Tanabe, T.M. Jessell, and F. Costantini. 2001. Cre reporter strains produced by targeted insertion of EYFP and ECFP into the ROSA26 locus. *BMC Dev. Biol.* 1:4.
17. Rubtsov, Y.P., J.P. Rasmussen, E.Y. Chi, J. Fontenot, L. Castelli, X. Ye, P. Treuting, L. Siewe, A. Roers, W.R. Henderson Jr., et al. 2008. Regulatory T cell-derived interleukin-10 limits inflammation at environmental interfaces. *Immunity.* 28:546–558.
18. Zhou, L., J.E. Lopes, M.M. Chong, I.I. Ivanov, R. Min, G.D. Victora, Y. Shen, J. Du, Y.P. Rubtsov, A.Y. Rudensky, et al. 2008. TGF-beta-induced Foxp3 inhibits T(H)17 cell differentiation by antagonizing RORgammat function. *Nature.* 453:236–240.
19. Wan, Y.Y., and R.A. Flavell. 2007. Regulatory T-cell functions are subverted and converted owing to attenuated Foxp3 expression. *Nature.* 445:766–770.
20. Pearce, E.L., A.C. Mullen, G.A. Martins, C.M. Krawczyk, A.S. Hutchins, V.P. Zediak, M. Banica, C.B. DiCioccio, D.A. Gross, C.A. Mao, et al. 2003. Control of effector CD8+ T cell function by the transcription factor Eomesodermin. *Science.* 302:1041–1043.
21. Djuretic, I.M., D. Levanon, V. Negreanu, Y. Groner, A. Rao, and K.M. Ansel. 2007. Transcription factors T-bet and Runx3 cooperate to activate Ifng and silence Il4 in T helper type 1 cells. *Nat. Immunol.* 8:145–153.
22. Chi, H., B. Lu, M. Takekawa, R.J. Davis, and R.A. Flavell. 2004. GADD45beta/GADD45gamma and MEKK4 comprise a genetic pathway mediating STAT4-independent IFNgamma production in T cells. *EMBO J.* 23:1576–1586.
23. Lin, W., D. Haribhai, L.M. Relland, N. Truong, M.R. Carlson, C.B. Williams, and T.A. Chatila. 2007. Regulatory T cell development in the absence of functional Foxp3. *Nat. Immunol.* 8:359–368.
24. Gavin, M.A., J.P. Rasmussen, J.D. Fontenot, V. Vasta, V.C. Manganiello, J.A. Beavo, and A.Y. Rudensky. 2007. Foxp3-dependent programme of regulatory T-cell differentiation. *Nature.* 445:771–775.
25. Wang, X. 2008. miRDB: A microRNA target prediction and functional annotation database with a wiki interface. *RNA.* 14:1012–1017.
26. Williams, L.M., and A.Y. Rudensky. 2007. Maintenance of the Foxp3-dependent developmental program in mature regulatory T cells requires continued expression of Foxp3. *Nat. Immunol.* 8:277–284.
27. Zheng, Y., S.Z. Josefowicz, A. Kas, T.T. Chu, M.A. Gavin, and A.Y. Rudensky. 2007. Genome-wide analysis of Foxp3 target genes in developing and mature regulatory T cells. *Nature.* 445:936–940.
28. Sarris, M., K.G. Andersen, F. Randow, L. Mayr, and A.G. Betz. 2008. Neuropilin-1 expression on regulatory T cells enhances their interactions with dendritic cells during antigen recognition. *Immunity.* 28:402–413.
29. Lee, E.C., D. Yu, J. Martinez de Velasco, L. Tessarollo, D.A. Swing, D.L. Court, N.A. Jenkins, and N.G. Copeland. 2001. A highly efficient *Escherichia coli*-based chromosome engineering system adapted for recombinogenic targeting and subcloning of BAC DNA. *Genomics.* 73:56–65.